Λ production in 4A GeV Carbon-nucleus interactions

A.Zinchenko, Yu.Gornaya, M.Kapishin, G.Pokatashkin, I.Rufanov, V.Vasendina

for the BM@N collaboration

VBLHEP, JINR, Dubna, Russia

Joint Institute for Nuclear Research

SCIENCE BRINGING NATIONS TOGETHER

BM@N DAC meeting
18.06.2019

Outline

1. Technical run with carbon beam (March 2017)
   - ✓ BM@N detector set-up
2. Data analysis (*C*+*C*, *C*+*Al*, *C*+*Cu* at 4A GeV)
   - ✓ Selection criteria
   - ✓ Reconstructed signal of Λ (dN/dy & dN/p_T spectra)
   - ✓ Data - MC agreement: multiplicity, momentum spectra
   - ✓ Decomposition of Λ reconstruction efficiency
   - ✓ Cross section and yields of Λ
   - ✓ Systematic errors and extrapolation factors
   - ✓ Reconstructed p_T spectra of Λ and extracted temperature
3. Summary

BM@N set-up in carbon run

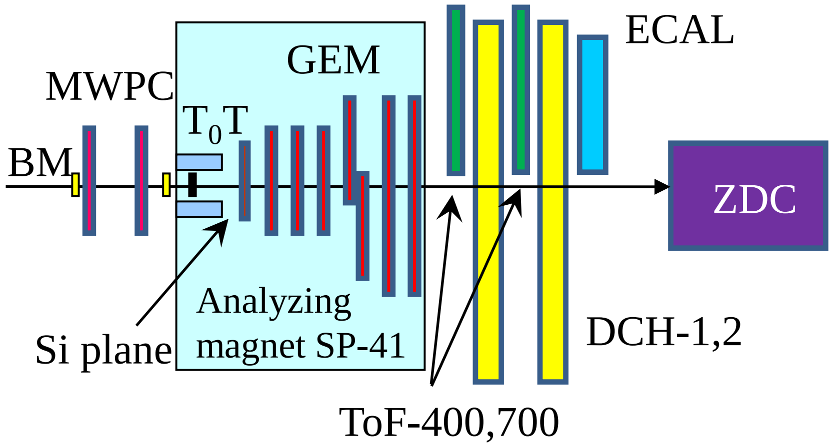

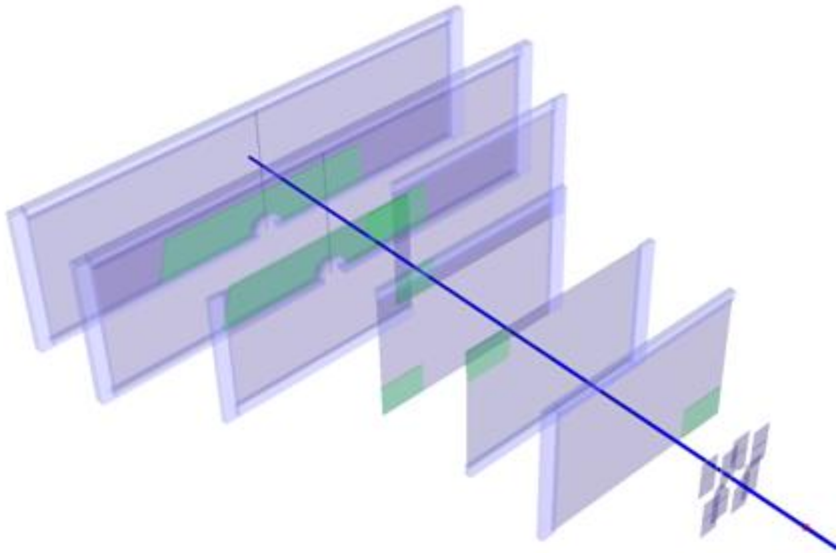

Central tracker in carbon run.

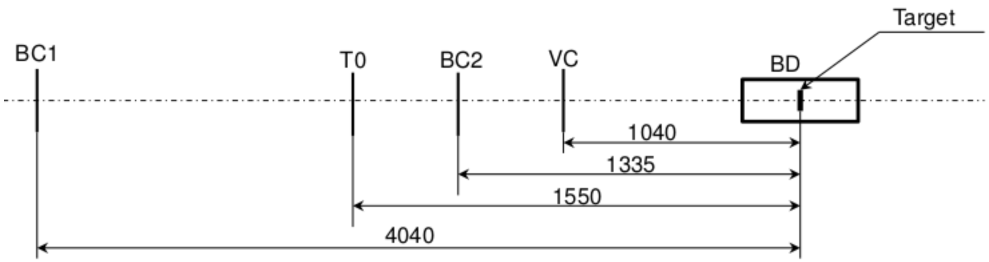

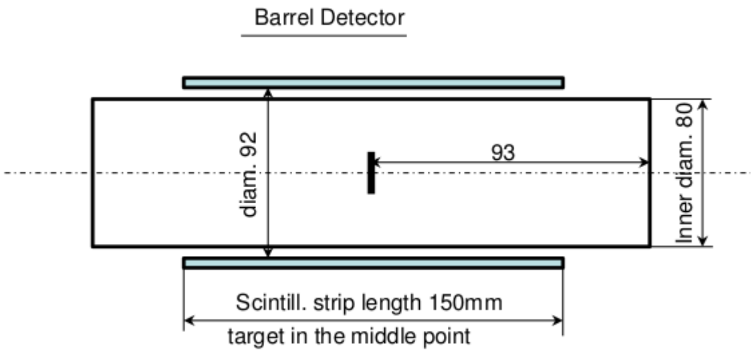

Schematic view and positions of the beam counters, barrel detector and target.

Event selection criteria

- ✓ Number of tracks in selected events: pos>=1, neg>=1;
- ✓ Beam halo, pile-up suppression within the readout time window: number of signals in the start detector: T0=1, number of signals in the beam counter: BC2=1, number of signals in the veto counter around the beam: Veto=0;
- ✓ Trigger condition in the barrel multiplicity detector: number of signals BD>=2 or BD>=3 (run dependent).

Cut	1	2	3	4
T0==1	+			+
BC2==1		+		+
Veto==0			+	+
C	77.0	82.7	82.1	67.4
Al	82.4	87.5	86.0	74.0
Cu	86.0	89.1	87.9	77.9

Table. Number of triggered events, beam fluxes and integrated luminosities collected in the carbon beam of 4A GeV.

Interactions (target thickness)	**Number of triggers / 10^6**	**Integrated beam flux / 10^7**	**Integrated luminosity / 10^{30} cm^{-2}**
C+C (9mm)	4.57	6.99	7.16
C+Al (12mm)	5.35	4.41	3.11
C+Cu (5mm)	5.31	4.57	1.98

Λ hyperon selection criteria

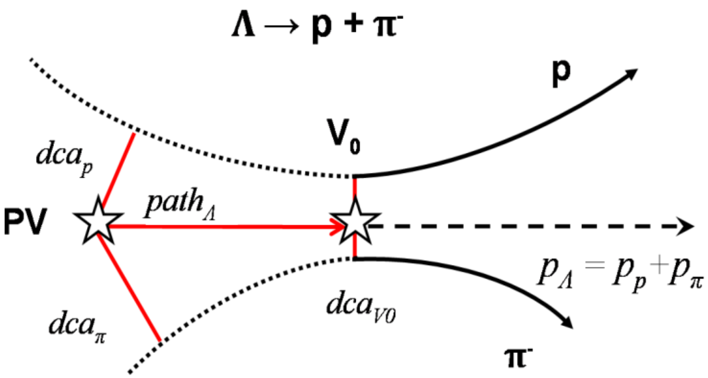

- ✓ Number of hits in 1 Si + 6 GEM per track > 3
- ✓ Momentum range of positive tracks: p_{pos}< 3.9 GeV/*c*
- ✓ Momentum range of negative tracks: p_{neg}>0.3 GeV/*c*
- ✓ Distance of minimum approach of *V0* tracks: *dca*< 1 cm
- ✓ Distance between *V0* and primary vertex: *path* > 2.5 cm

Event topology:

- ✓ PV – primary vertex
- ✓ V_0 – vertex of hyperon decay
- ✓ *dca* – distance of the closest approach
- ✓ *path* – decay length

Table. Reconstructed signals of *Λ* in p_T and *y* bins. The first error presents the statistical uncertainty, the second error is systematical.

Target / Interval	*Y*			Target / Interval	p_T		
	C	***Al***	***Cu***		***C***	***Al***	***Cu***
1.2-1.45	103±27±18	265±45±30	591±69±46	0.1-0.3	454±68±46	652±84±56	625±85±58
1.45-1.65	250±43±29	510±59±38	601±60±39	0.3-0.55	296±44±29	717±80±53	797±81±54
1.65-1.85	338±57±38	550±72±48	576±77±52	0.55-0.8	128±31±20	462±65±43	379±61±41
1.85-2.1	253±51±35	443±72±49	371±67±45	0.8-1.05	N/A	96±39±27	133±44±30

Signal of Λ in *C+Cu* interaction

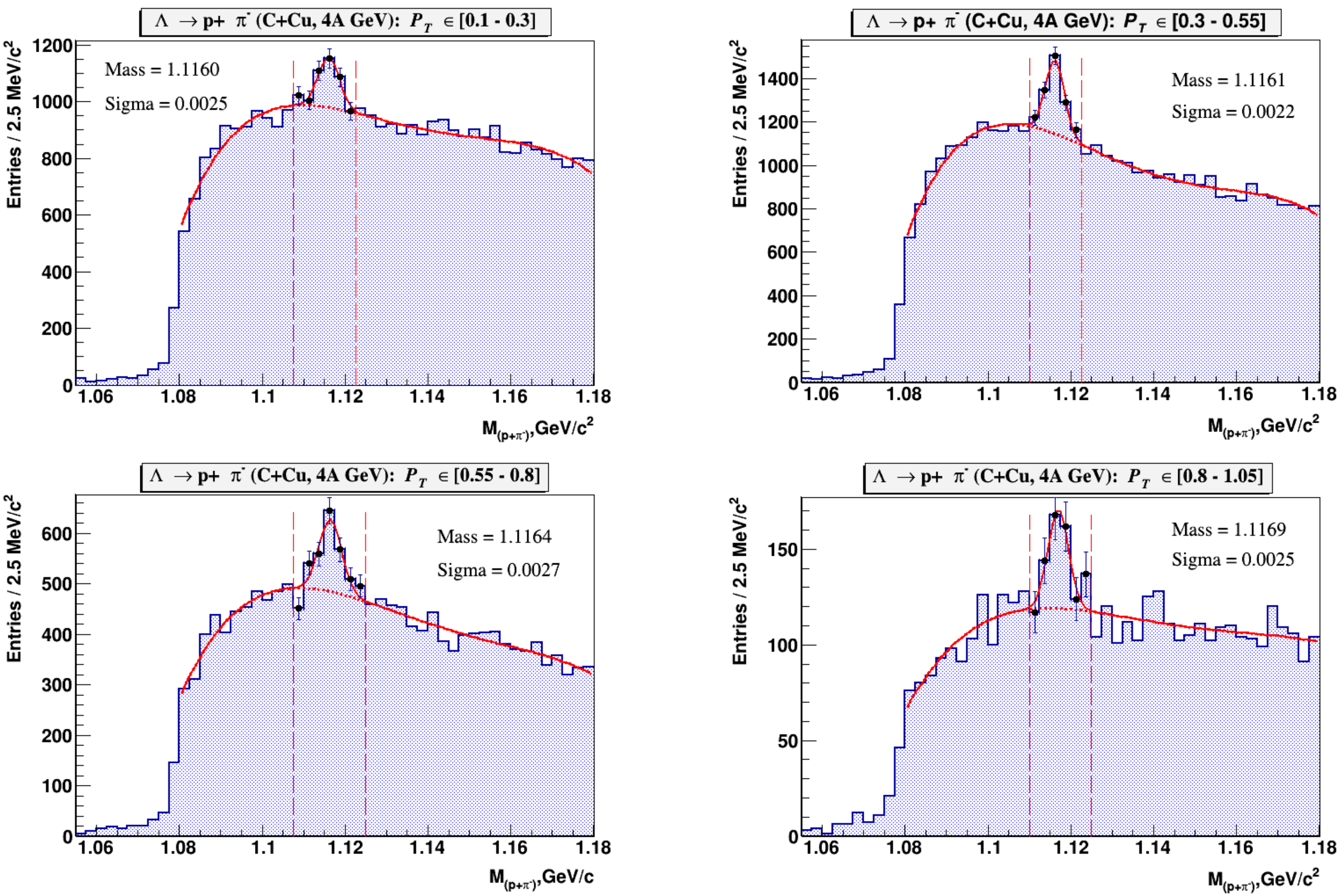

Fig. $\Lambda\rightarrow p\pi^-$ signal reconstructed in *C+Cu* interaction in bins of the transverse momentum p_T. The signal is fitted by a Gaussian function, the background is fitted by the 4th degree polynomial.

Signal of Λ in $C+Cu$ interaction

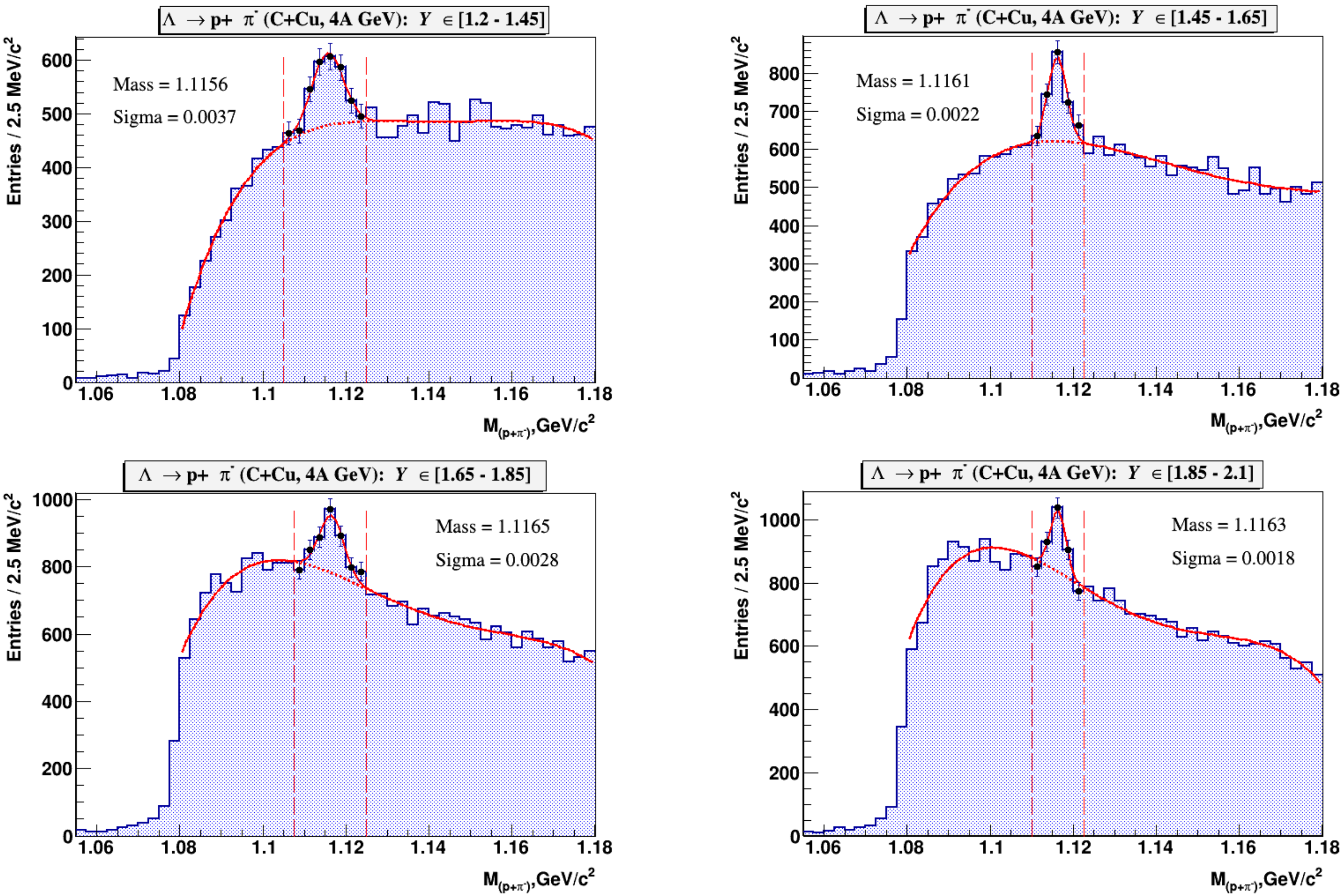

Fig. $\Lambda \rightarrow p\pi^-$ signal reconstructed in $C+Cu$ interaction in bins of the rapidity y. The signal is fitted by a Gaussian function, the background is fitted by the 4th degree polynomial.

Signal of Λ in *C+C*, *C+Al*, *C+Cu* interactions

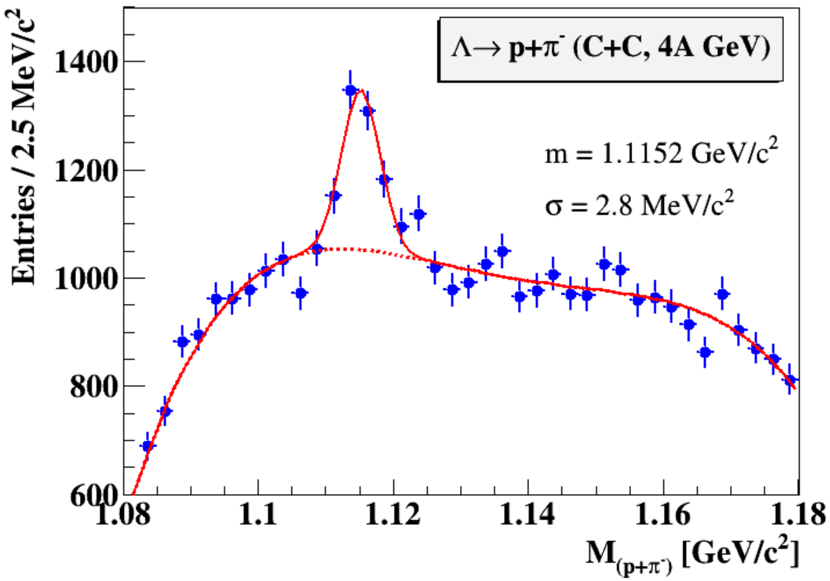

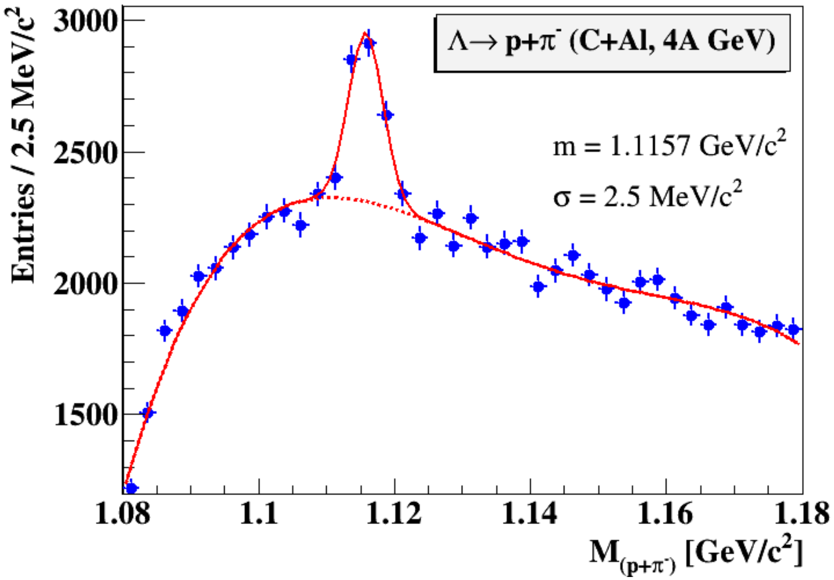

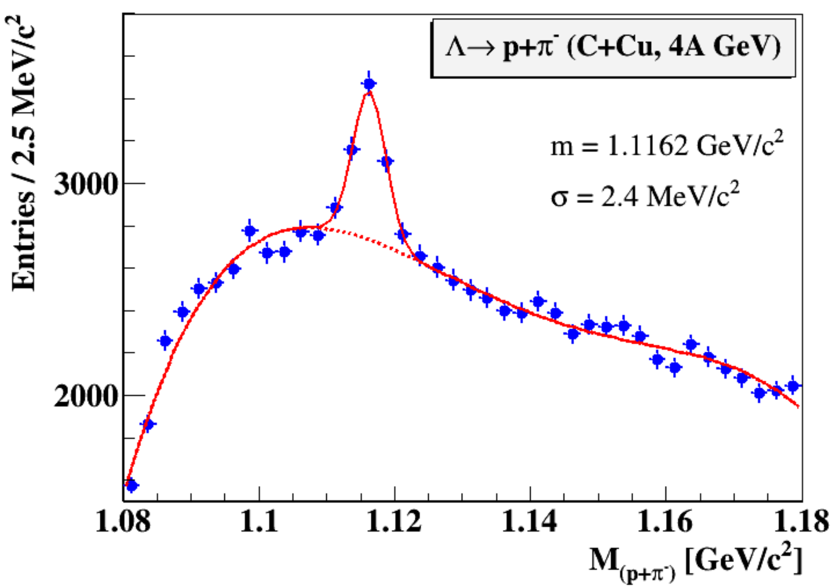

Fig. $\Lambda \to p\pi^-$ signal reconstructed in interactions of the carbon beam with targets: *C*, *Al*, *Cu*.

Variation of sigma

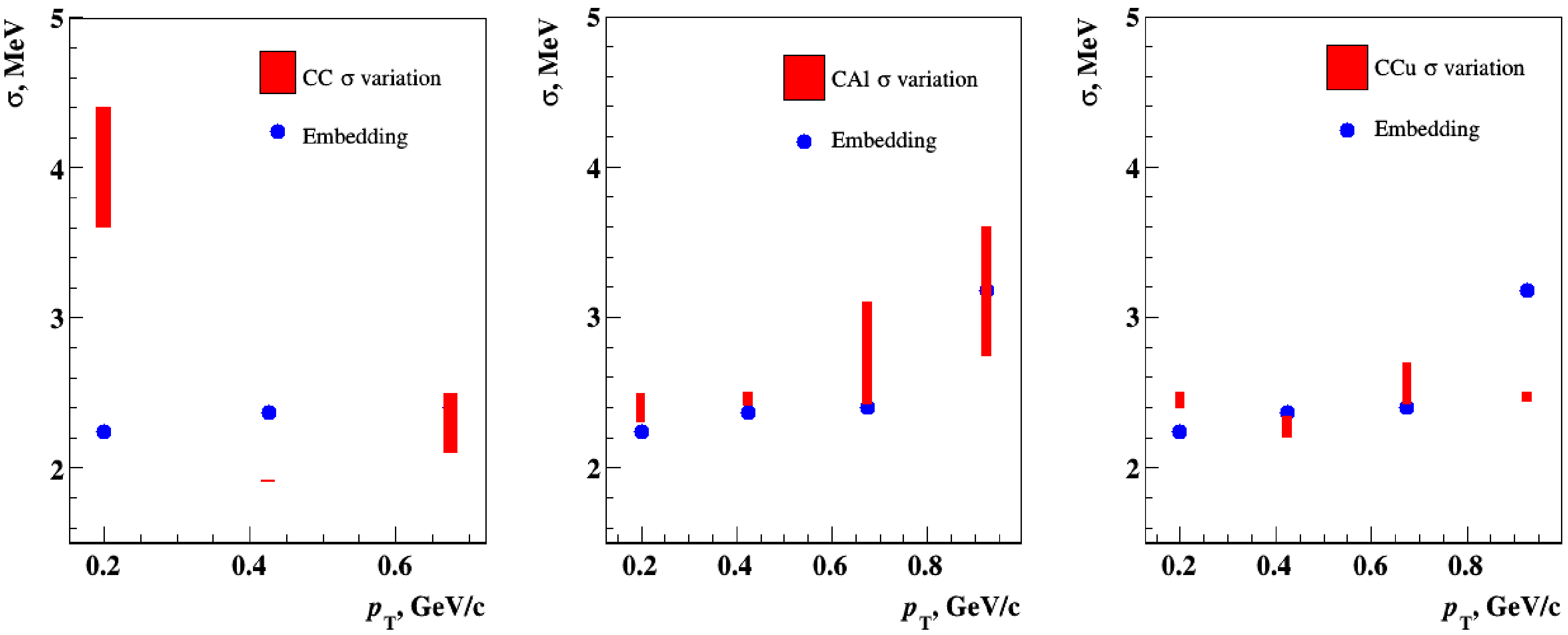

Fig. Variation of sigma of the experimental Λ and embedded Λ signals reconstructed in bins of p_T in *C+C*, *C+Al*, *C+Cu* interactions. To estimate statistical fluctuations of the experimental Λ signal, the Gaussian fit is performed for the mass distribution shifted at a half of the mass bin (1.25 MeV/c^2). The difference in sigma is presented as an error band.

Number of reconstructed Λ hyperons

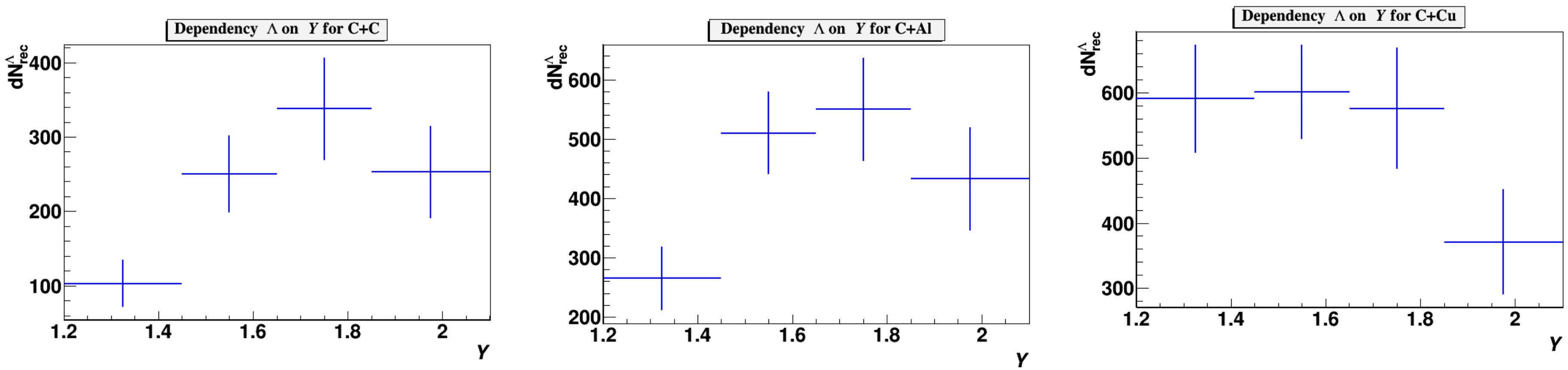

Fig.15. Number of reconstructed *Λ* hyperons in *C+C*, *C+Al*, *C+Cu* data samples in bins of *y*.

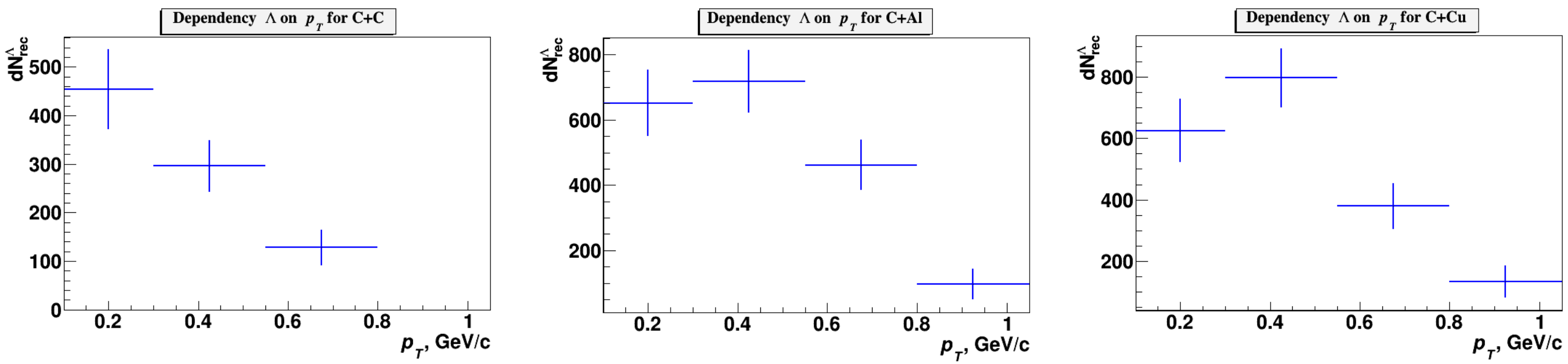

Fig. Number of reconstructed *Λ* hyperons in *C+C*, *C+Al*, *C+Cu* data samples in bins of p_T.

Comparison of experimental data and MC

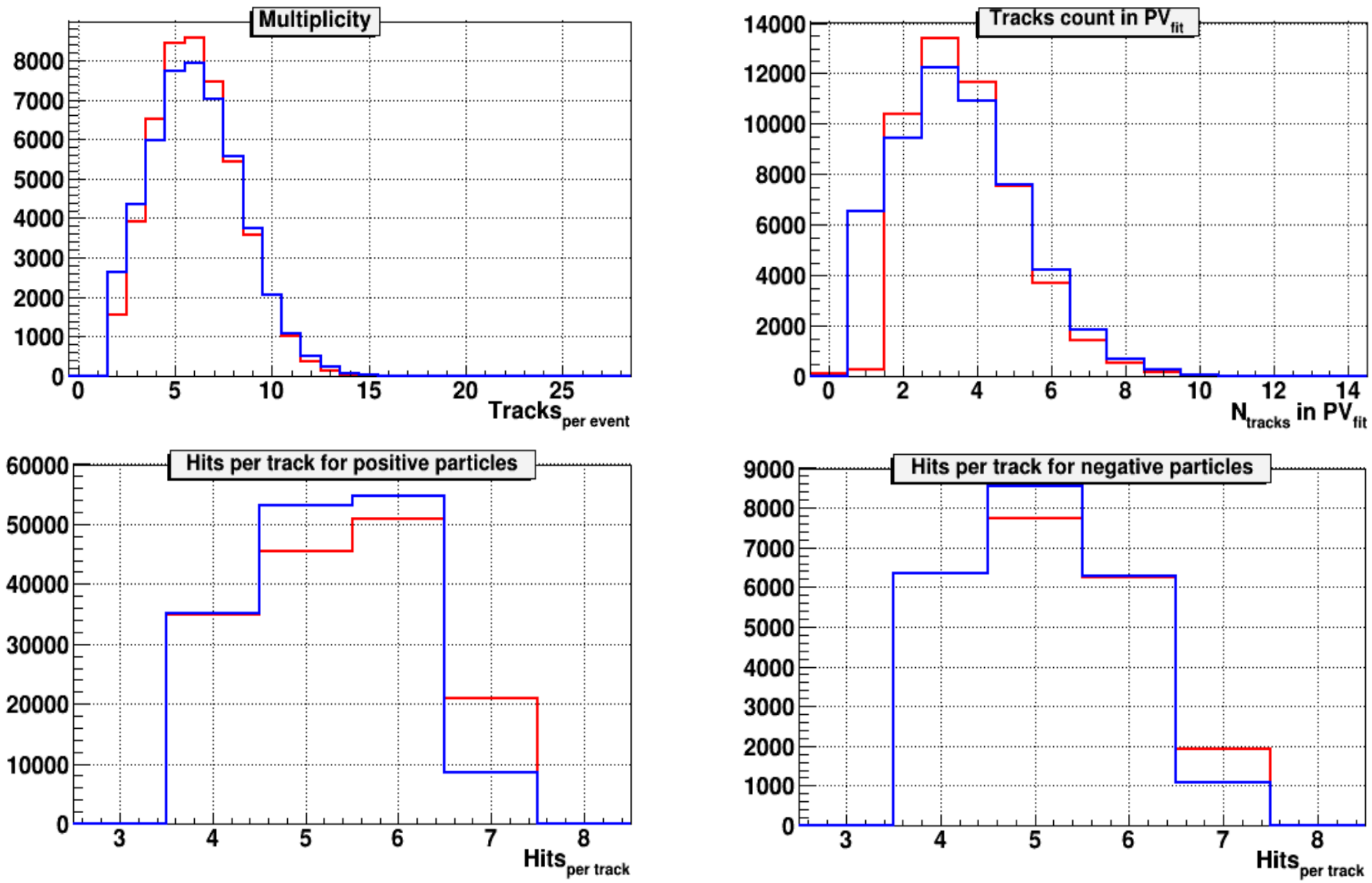

Fig. Comparison of experimental distributions (red lines) and MC (DCM-QGSM) (blue curves) in *C+Cu* interaction: track multiplicity per event; number of tracks reconstructed in the primary vertex; number of hits per positive particle reconstructed in 1 Si + 6 GEM detectors; number of hits per negative particle.

Comparison of experimental data and MC

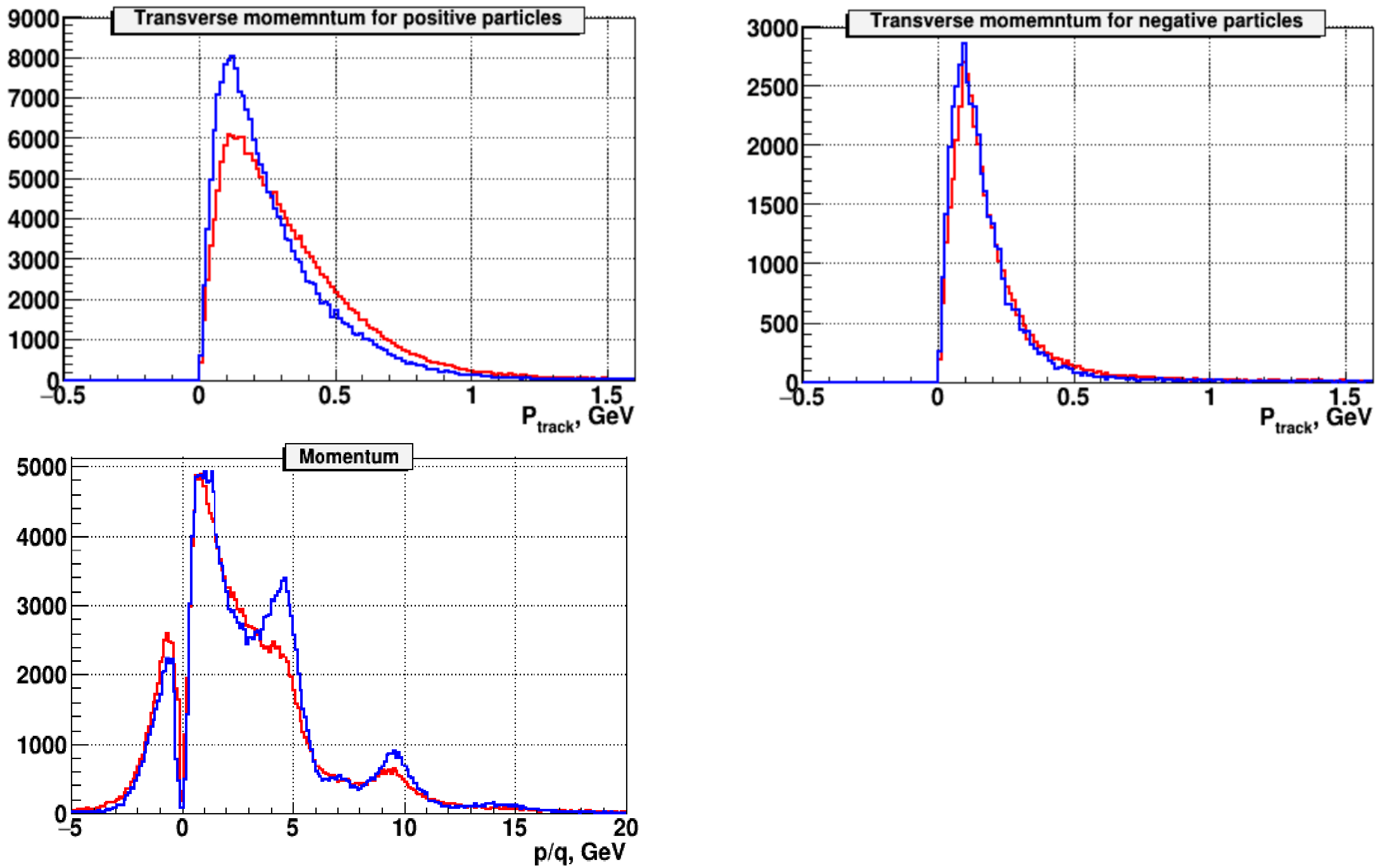

Fig. Comparison of experimental data (red curves) and MC (DCM-QGSM) simulation (blue curves) in *C+Cu* interaction: transverse momentum of positive particles; transverse momentum of negative particles; total momentum of negative (*p/q*<0) and positive particles (*p/q*>0).

Decomposition of efficiency

Table. Decomposition of Λ reconstruction efficiency.

Reconstruction efficiency	$\varepsilon_{rec} = \varepsilon_{acc} \cdot \varepsilon_{emb} \cdot \varepsilon_{cuts}$
Λ geometrical acceptance in GEM detectors	$\varepsilon_{acc} = N_{acc}(y,p_T) / N_{gen}(y,p_T)$
Efficiency of reconstruction of embedded Λ	$\varepsilon_{emb} = N_{emb}(y,p_T) / N_{acc}(y,p_T)$
Efficiency of Λ selection: kinematical and spatial cuts	$\varepsilon_{cuts} = N_{rec}(y,p_T) / N_{emb}(y,p_T)$

Efficiency in $C+Cu$ interaction

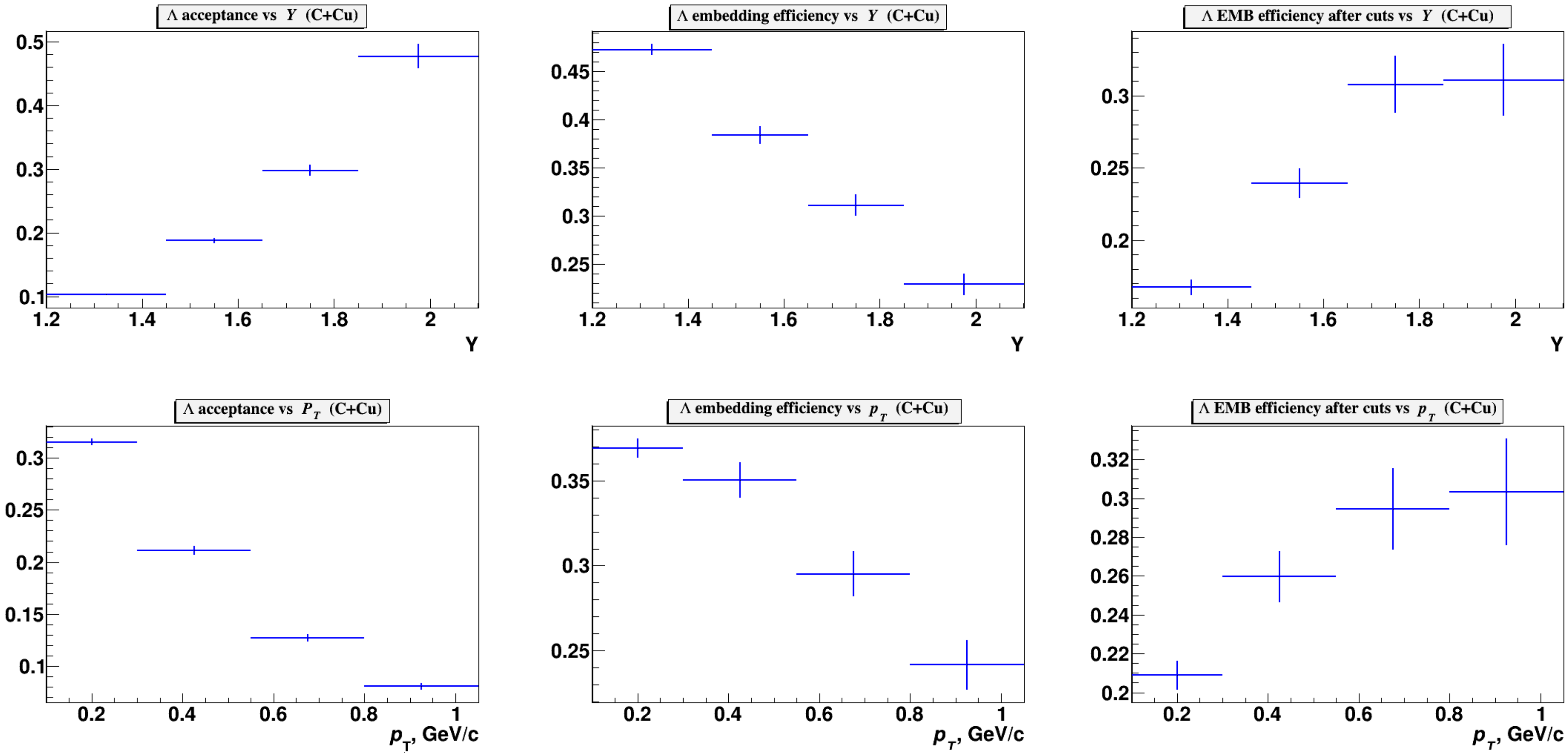

Fig. Λ geometrical acceptance (ε_{acc}); efficiency of reconstruction of embedded Λ (ε_{emb}); efficiency of kinematical and spatial cuts applied for Λ reconstruction (ε_{cuts}) as functions of rapidity y (top plots) and p_T (bottom plots). Results are shown for $C+Cu$ interaction.

Cross section and yields of Λ hyperon

The cross section σ_Λ and yield Y_Λ of Λ hyperon production in *C+C*, *C+Al*, *C+Cu* interactions are calculated in bins of y and p_T according to the formulae:

$$\sigma_\Lambda(y,p_T)=N_{rec}^{\Lambda}(y,p_T) / (\varepsilon_{rec}(y,p_T)\cdot\varepsilon_{trig}\cdot L); \qquad Y_\Lambda(y,p_T) = \sigma_\Lambda(y,p_T) / \sigma_{inel}$$

where L is the luminosity,
N_{rec}^{Λ}–the number of reconstructed Λ hyperons,
ε_{rec}–the combined efficiency of the Λ hyperon reconstruction,
ε_{trig}–the trigger efficiency,
σ_{inel}– the cross section for minimum bias inelastic *C+A* interactions.

Interaction	***C+C***	***C+Al***	***C+Cu***
Inelastic cross section, mb	830±50	1260±50	1790±50

The cross sections for inelastic *C+Al*, *C+Cu* interactions are taken from the predictions of the DCM-QGSM model which are consistent with the results calculated by the formula: $\sigma_{inel} = \pi R_0^2 (A_P^{1/3} + A_T^{1/3})^2$, where R_0 = 1.2 fm is an effective nucleon radius, A_P and A_T are atomic numbers of the beam and target nucleus.

Systematic errors

Table. Systematic uncertainty of the embedding efficiency.

Target / Interval	*y*			Target / Interval	p_T		
	C, sys%	***Al***, sys%	***Cu***, sys%		***C***, sys%	***Al***, sys%	***Cu***, sys%
1.2-1.45	2.09	4.22	2.93	**0.1-0.3**	4.94	9.37	6.61
1.45-1.65	1.75	4.11	3.31	**0.3-0.55**	3.07	0.64	1.30
1.65-1.85	7.96	4.78	4.19	**0.55-0.8**	4.59	0.34	0.08
1.85-2.1	5.44	1.24	6.09	**0.8-1.05**	3.03	6.28	2.36

Table. Systematic uncertainty of the total reconstruction efficiency.

Target / Interval	*y*			Target / Interval	p_T		
	C, sys%	***Al***, sys%	***Cu***, sys%		***C***, sys%	***Al***, sys%	***Cu***, sys%
1.2-1.45	2.09	4.22	2.93	**0.1-0.3**	4.94	9.37	6.61
1.45-1.65	1.75	4.11	3.31	**0.3-0.55**	3.07	0.64	1.30
1.65-1.85	7.96	4.78	4.19	**0.55-0.8**	4.59	0.34	0.08
1.85-2.1	5.44	1.24	6.09	**0.8-1.05**	3.03	6.28	2.36

Systematic errors

Table. Total systematic uncertainty.

Target / Interval	y			Target / Interval	p_T		
	C, sys%	***Al***, sys%	***Cu***, sys%		***C***, sys%	***Al***, sys%	***Cu***, sys%
1.2-1.45	19.0	14.8	10.5	**0.1-0.3**	14.2	15.1	12.7
1.45-1.65	14.1	10.6	8.0	**0.3-0.55**	10.7	9.6	8.6
1.65-1.85	16.5	12.5	10.8	**0.55-0.8**	19.8	14.0	11.3
1.85-2.1	16.6	13.3	14.4	**0.8-1.05**	N/A	29.7	22.7
Normalization	6.0	4.0	2.8	Normalization	6.0	4.0	2.8

Ratio of impact parameter distributions

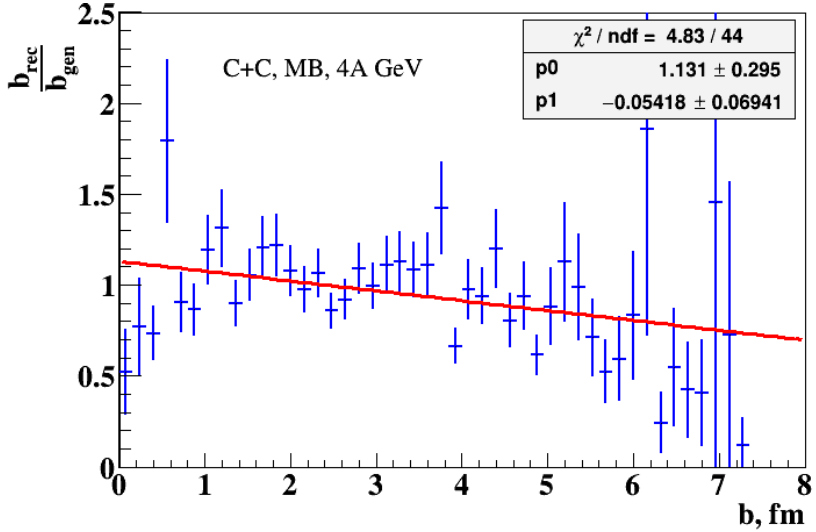

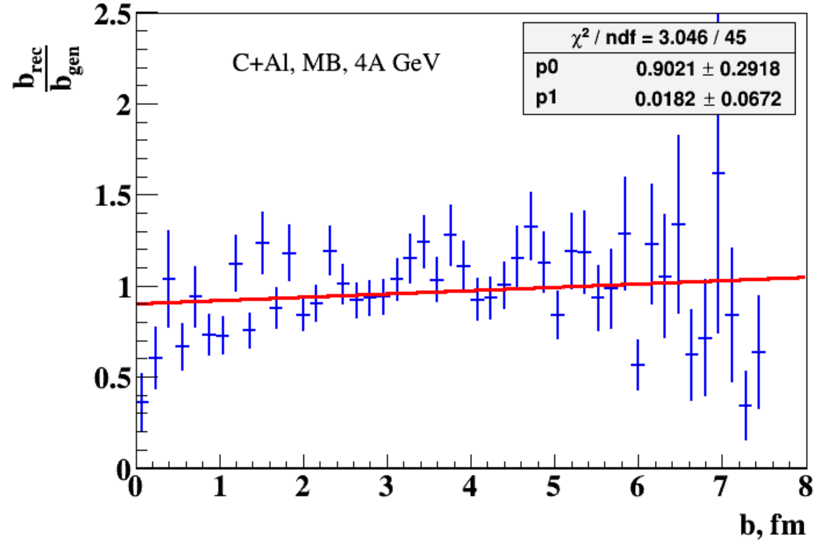

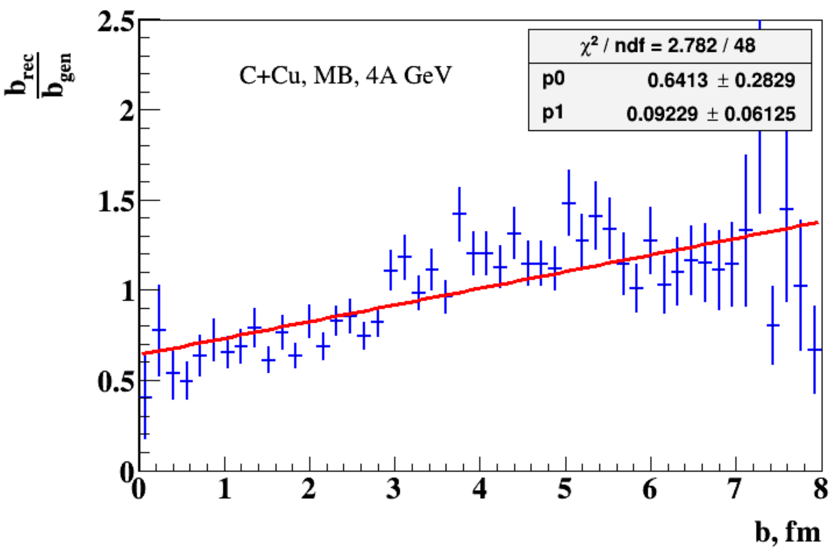

Fig. Ratio of impact parameter distributions for events with reconstructed Λ to events with generated Λ presented for *C+C, C+Al, C+Cu* interactions. Linear fit of the distributions is superimposed.

Reconstructed yields of Λ hyperons

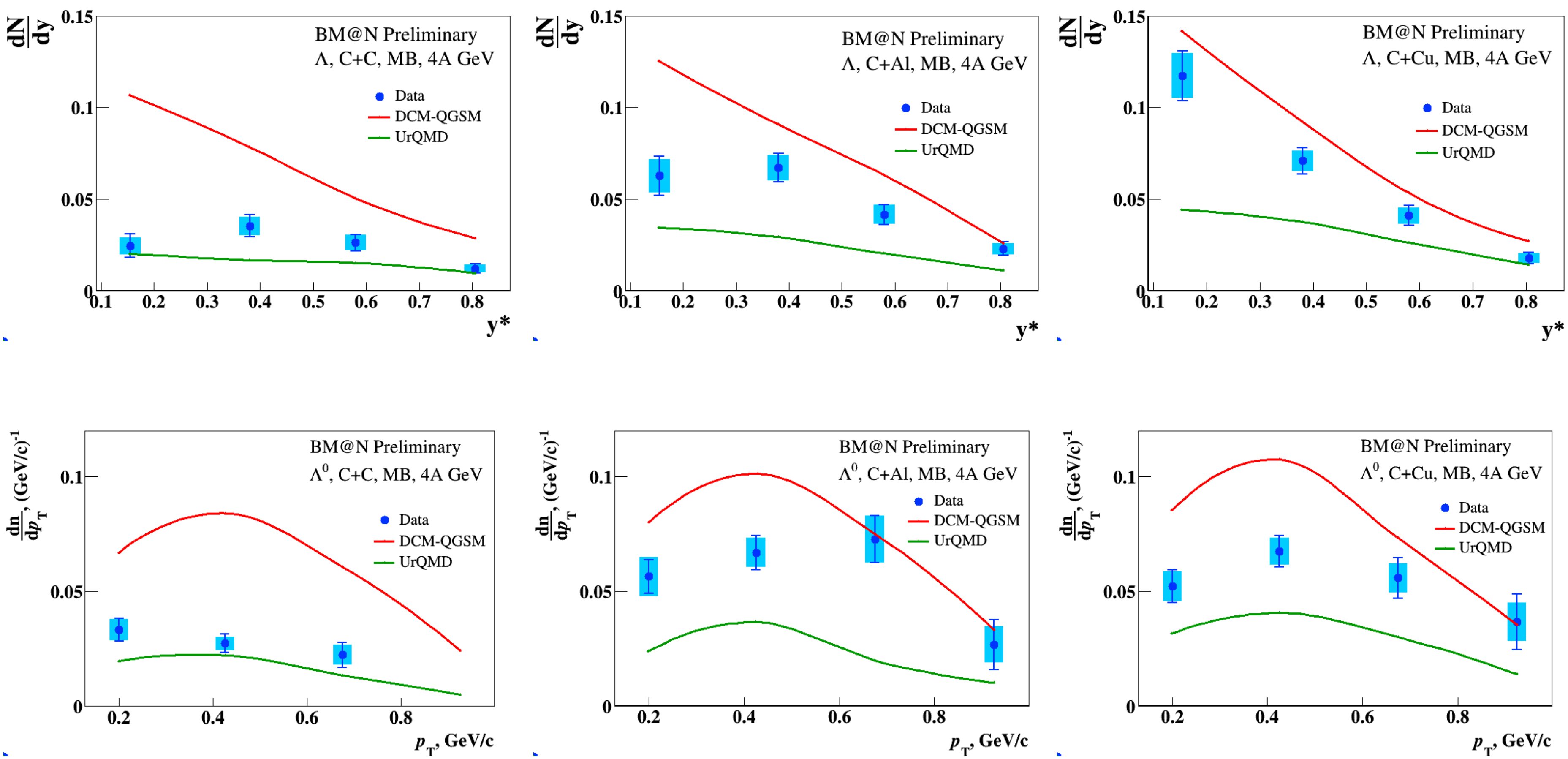

Fig. Reconstructed yields of *Λ* hyperons in minimum bias *C+C*, *C+Al*, *C+Cu* interactions vs rapidity *y* and transverse momentum p_T.

Reconstructed p_T spectra of Λ and extracted T_0

Table. Temperature parameter extracted from the fit of the p_T spectra.

	T_0, MeV (C+C)	T_0, MeV (C+Al)	T_0, MeV (C+Cu)
Experiment	98 ± 24 ± 25	157 ± 24 ± 12	160 ± 27 ± 21
χ^2 /ndf	2.04/1	2.51/2	0.39/2
DCM-QGSM	122	129	131
UrQMD	107	127	132

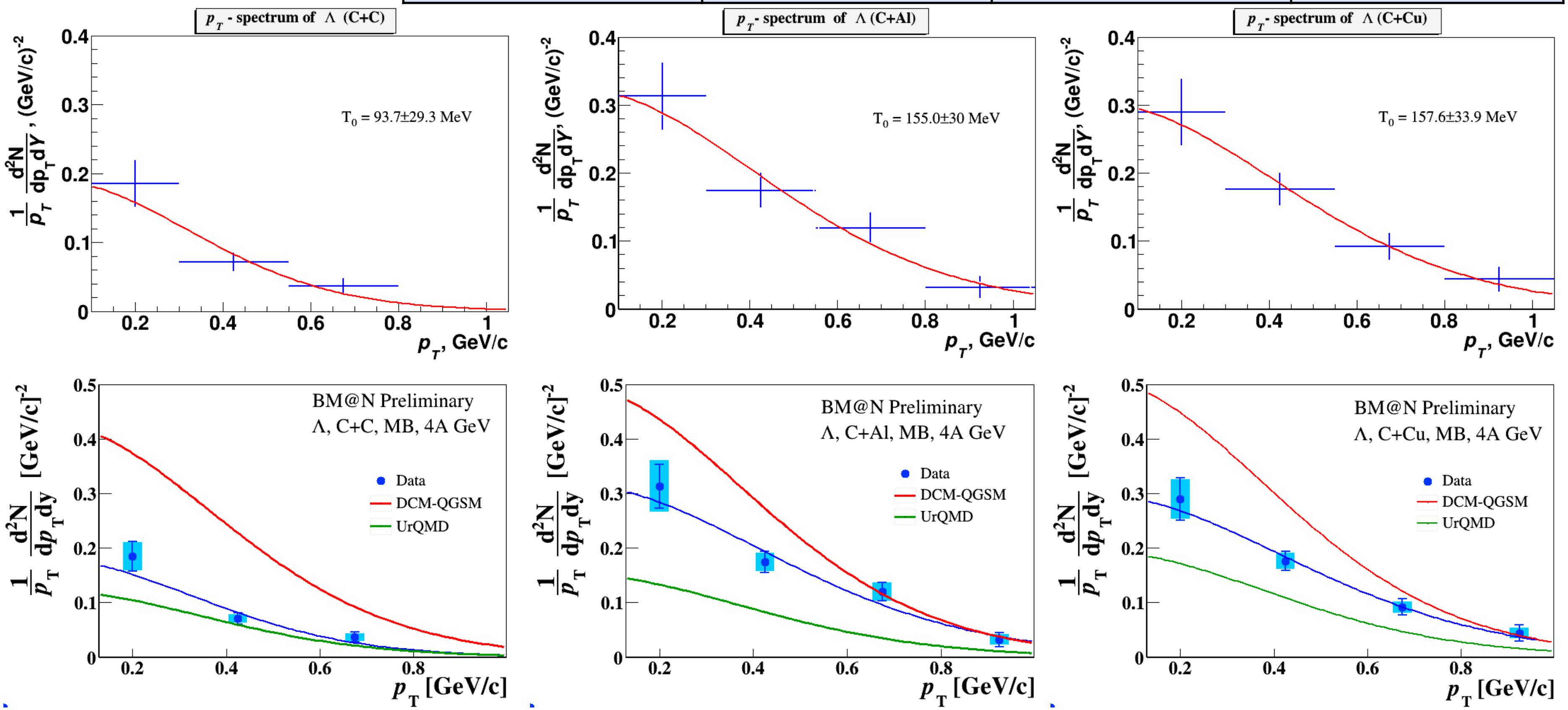

Fig. Thermal fit results with the inverse slope parameter T_0: data and predictions of models.

p_T spectra of Λ: MC predictions

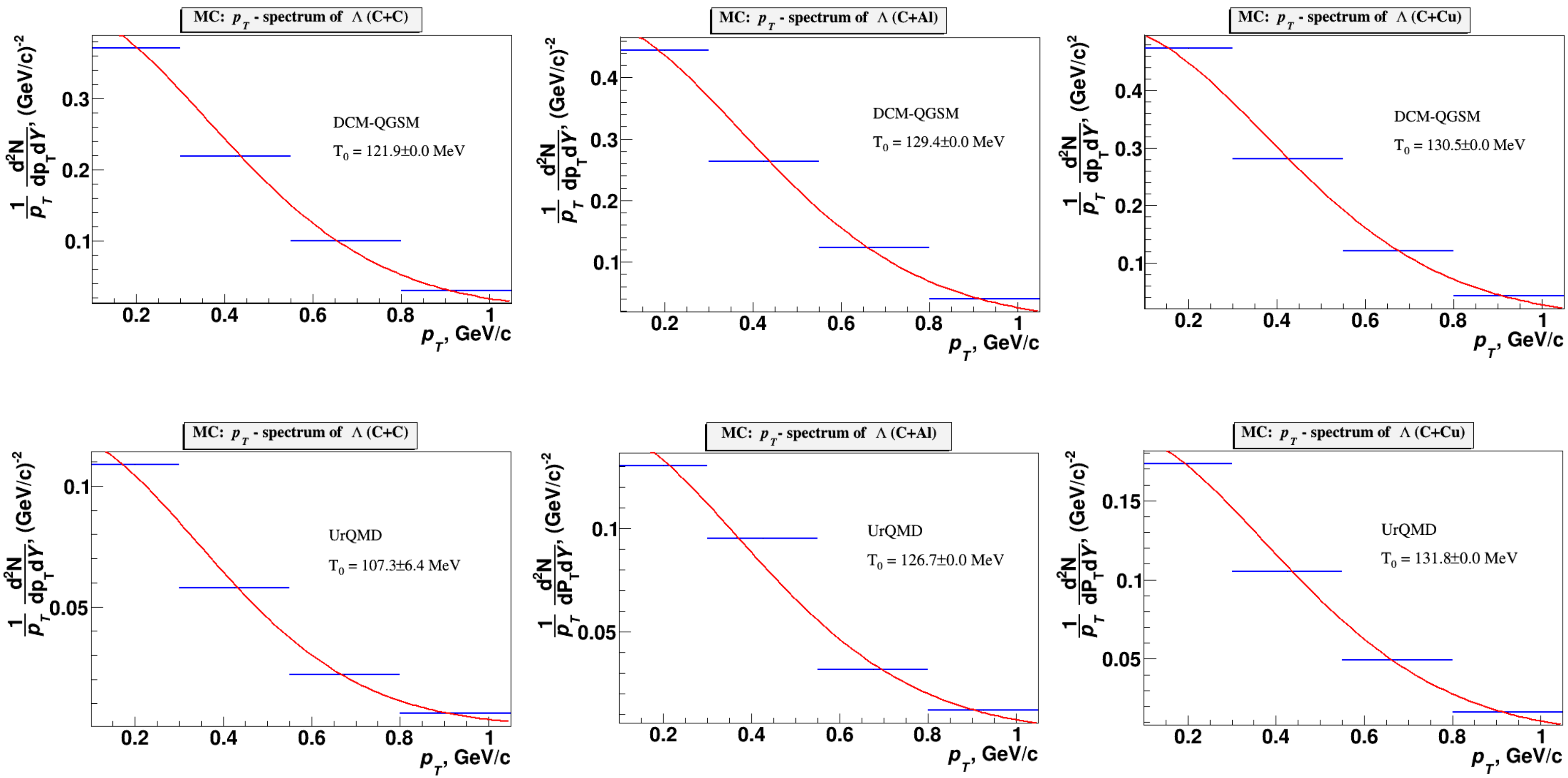

Fig. Fit of the DCM-QGSM and URQMD spectra. The inverse slope parameter T_0 is shown, extracted from the fit.

Extrapolation factors

Table. Extrapolation factors to the full kinematic range, yields and cross sections.

	C	***Al***	***Cu***
DCM-QGSM URQMD extrapolation factors	6574/2474 1827/639	10539/3413 3248/1056	15817/3545 5509/1360
Yields in the measured kin range $0.1<p_T<1.05$ GeV/c, $1.2<y_{lab}<2.1$	0.0214±0.0023±0.0024	0.0431±0.0034±0.0035	0.0561±0.0039±0.0047
Yields in the full kinematic range N part DCM-QGSM	0.0589±0.0063±0.0065 9	0.133±0.010±0.011 13.4	0.239±0.017±0.020 23
Λ cross section in min. bias interactions, mb	48.9 ± 5.2 ± 5.1	167 ± 13 ± 13	427 ± 30 ± 29

The Λ yields and production cross section

Interacting nucleus / reference	**Beam momentum, kinetic energy (T_0)**	***Λ* cross section, mb**	***Λ* yield, $\cdot 10^{-2}$**
He_4+Li_6	4.5 GeV/c (3.66A GeV)	5.9± 1.5	1.85 ± 0.5
C+C	4.2 GeV/c (3.36AGeV)	24 ± 4	
C+C, propane chamber	4.2 GeV/c (3.36A GeV)		2.8 ± 0.3
p+p	4.95 GeV/c (4.1 GeV)		2.3 ± 0.4
C+C, HADES	2A GeV	$8.7 \pm 1.1 \pm^{3.2}_{1.6}$	$0.92 \pm 0.12 \pm^{0.34}_{0.17}$
Ar+KCl, HADES	1.76AGeV		3.93±0.14±0.15
Ar+KCl, FOPI	1.93A GeV		3.9±0.14±0.08
Ni+Ni, FOPI, central 390 mb from 3.1 *b*	1.93A GeV		$0.137 \pm 0.005 \pm^{0.009}_{0.025}$
Ni+Cu, EOS, full *b*<8.9 fm / central *b*<2.4 fm	2A GeV	112±24 / 20±3	
Ar+KCl, central *b*<2.4 fm	1.8A GeV	7.6±2.2	

Energy dependence of Λ yields

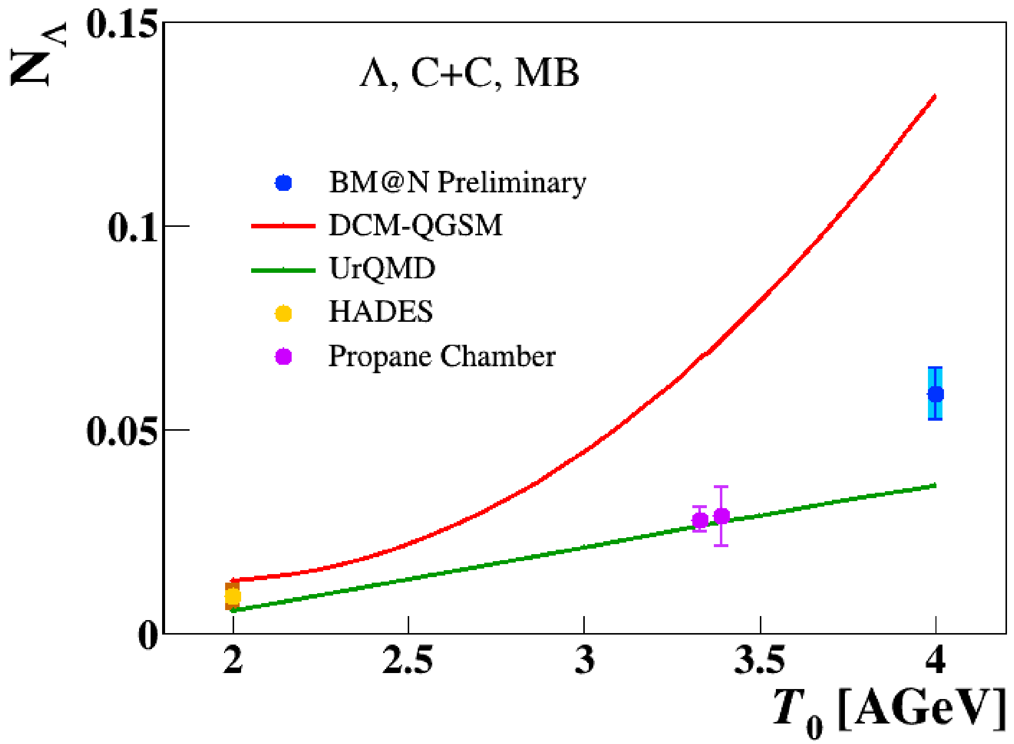

Fig. Energy dependence of *Λ* yields measured in different experiments. BM@N result is compared with data [*S.Arakelian et al., P1-83-354, JINR, Dubna; D.Armutlijsky et al., P1-85-220, JINR, Dubna; Kalliopi Kanaki, PhD "Study of Λ hyperon production"*]. The predictions of the DCM-QGSM and UrQMD models are shown.

Summary

1. Production of Λ hyperons in interactions of the 4A GeV kinetic energy carbon beam with *C*, *Al*, *Cu* targets was studied with the BM@N detector at the Nuclotron.
2. The analysis procedure has been presented and described.
3. Results on Λ hyperon yields have been obtained and compared with model predictions and data available.

Thank you for attention!

Backup

Triggers and impact parameters

Table. Trigger efficiency evaluated for events with reconstructed *Λ* hyperons in interactions of the carbon beam with *C*, *Al*, *Cu* targets. The systematic errors take into account the uncertainty due to the delta electron background. The last row shows the trigger efficiency averaged over the data samples with trigger conditions BD>=2 and BD>=3.

Trigger / Target	*C*	*Al*	*Cu*
ε_{trig} (BD>=2)	0.906±0.010	0.955±0.010	0.904±0.01
ε_{trig} (BD>=3)		0.923±0.020	0.883±0.02
ε_{trig} averaged		0.940±0.015	0.893±0.015

Table. Mean impact parameters of min. bias *C+C*, *C+Al*, *C+Cu* interactions.

MC	*b*, fm (*C+C*)	*b*, fm (*C+Al*)	*b*, fm (*C+Cu*)
All min bias events	3.76	4.36	5.13
Events with gen. *Λ*	2.80	3.08	3.58
Events with rec. *Λ*	2.71	3.18	3.88

Residual distributions of GEM hits

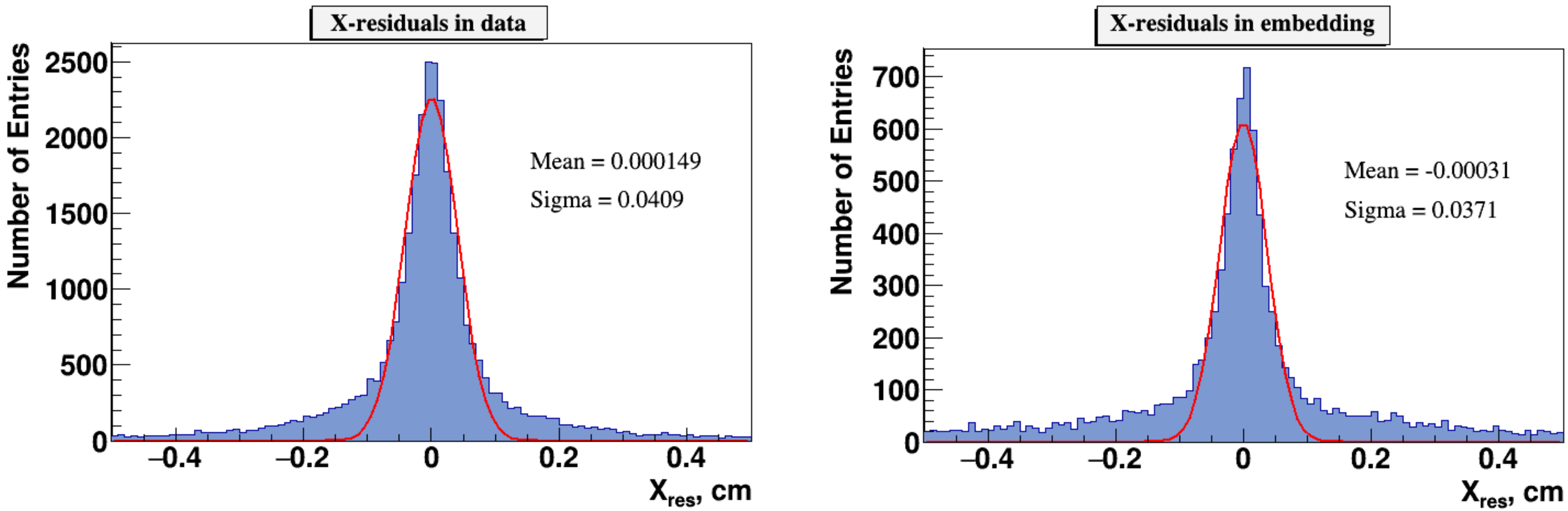

Fig. 12. Residual distributions of GEM hits with respect to reconstructed tracks: left) experimental data, right) reconstructed tracks of embedded *Λ* decay products.

DCA and PV position

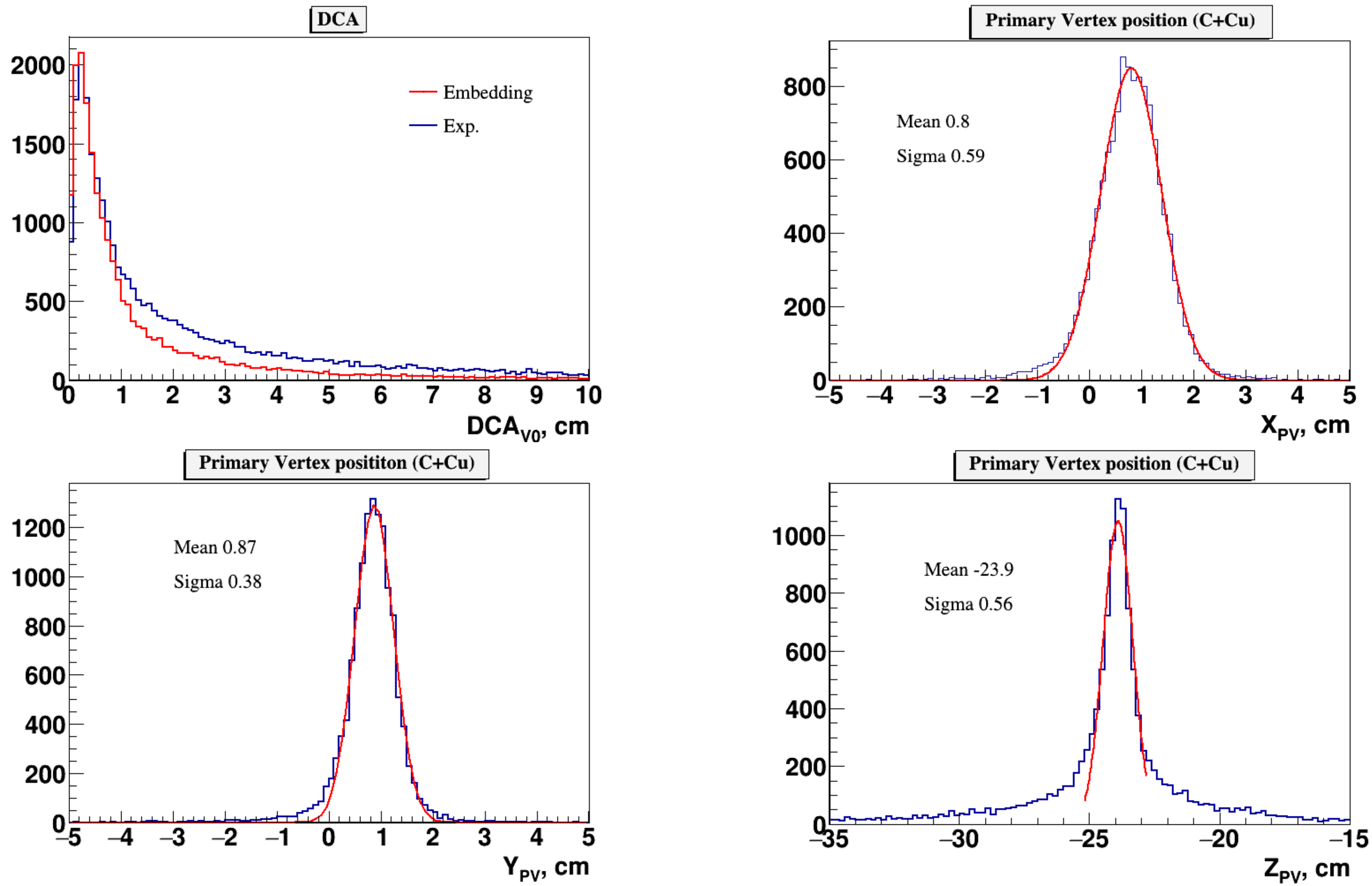

Fig. 12b. Distance of the closest approach of *V0* decay tracks (*DCA*) and *Z*,*X*,*Y* distributions of the primary vertex.

Path and momentum distribution

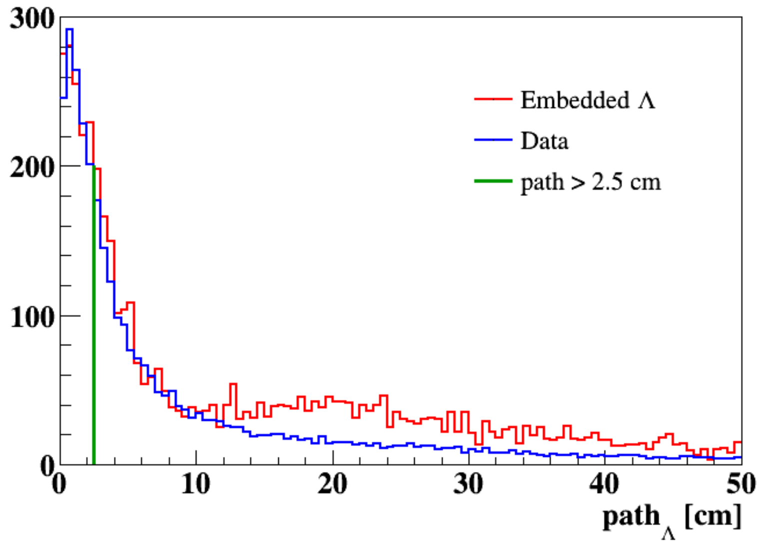

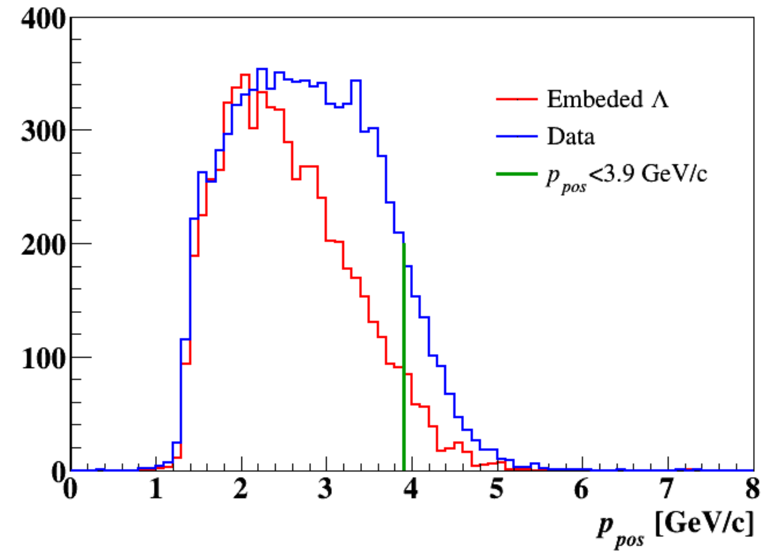

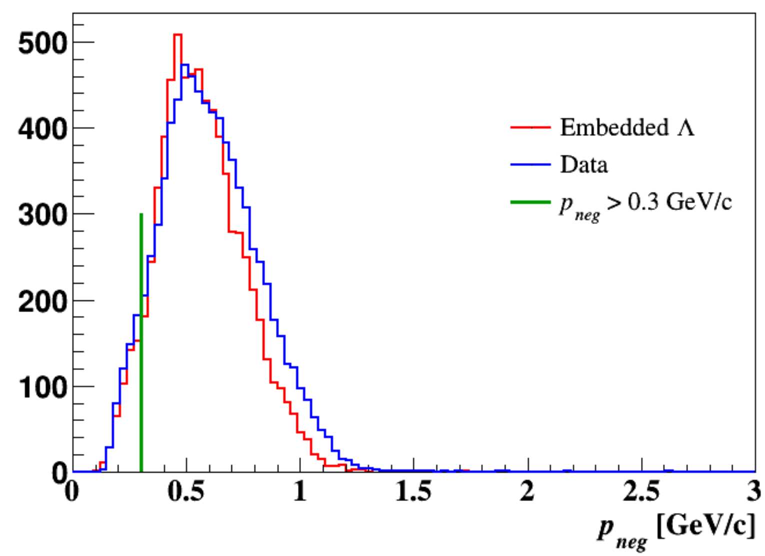

Fig. Path, momentum distributions of positive, negative tracks from *V0* decays. Experimental data are compared with distributions for embedded *Λ* hyperons.

The invariant mass spectrum

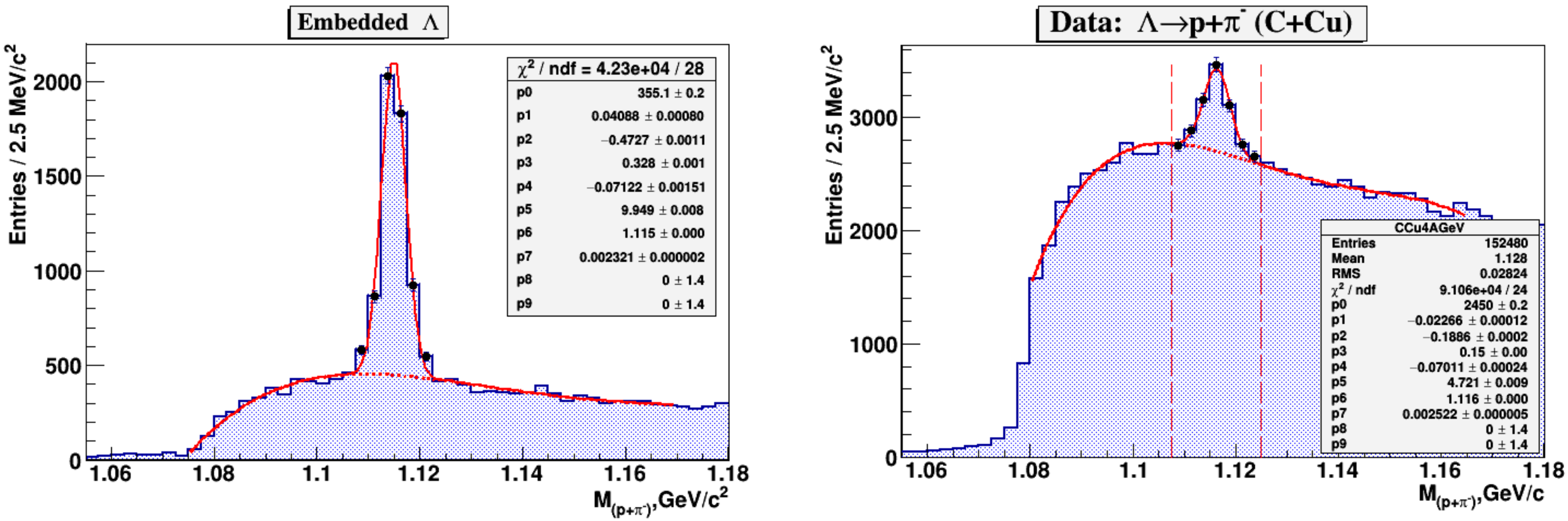

Fig. 13. The invariant mass spectrum of (p,π^-) pairs reconstructed in the experimental events of $C+Cu$ interactions with embedded Λ hyperon decay products (left); The invariant mass spectrum of (p,π^-) pairs reconstructed in $C+Cu$ interactions (right).